Eur. Phys. J. B **4**, 205–217 (1998)

THE EUROPEAN PHYSICAL JOURNAL B

Effects of ionic strength and charge annealing in star-branched polyelectrolytes

O.V. Borisov[1,a,b] and E.B. Zhulina[2,a]

[1] University of Wageningen, Department of Physical and Colloid Chemistry, 6703 HB Wageningen, The Netherlands
[2] University of Pittsburgh, Department of Chemical Engineering, Pittsburgh PA 15261, USA

Received: 10 November 1997 / Revised: 16 February 1998 / Accepted: 1st April 1998

Abstract. We have developed a scaling theory that describes the conformations of weak star-branched polyelectrolytes in dilute solutions. The dependences of the overall star size on the number of branches and on the ionic strength of the solution (tuned by the addition of low molecular weight salt) are analyzed. The intrinsic structure of the polyelectrolyte stars in salt-free and salt-added solutions is discussed in terms of concentration and elastic blobs. In contrast to neutral stars, the swollen corona of the polyelectrolyte star consists of blobs which are not closely packed. We have shown that the size of star polyelectrolytes is less sensitive to the variation in the ionic strength than the size of linear polyelectrolytes. The effects of the ionization-recombination balance in the star polyelectrolyte were taken into account. For polyelectrolytes with small ionization constant, the size of the star depends nonmonotonically on the number of branches and on the ionic strength of the solution due to recombination of counterions with charged monomers.

PACS. 36.20.Ey Conformation (statistics and dynamics) – 61.25.Hq Macromolecular and polymer solutions; polymer melts; swelling

1 Introduction

Currently, the general picture of polyelectrolyte solutions is still far from complete [1,2]. The main difficulties which arise in the theoretical analysis of solutions of charged macromolecules are related to the long-range character of Coulomb interactions and to the essentially nonlinear character of screening of large (and highly charged) polyions by small mobile counterions. The latter is manifested in the failure of the Debuy-Hückel approximation in application to the solution of polyelectrolytes, especially at low salt concentrations.

The interest in branched polyelectrolytes is initiated by both theoretical and practical reasons. In practice, the branched polyelectrolytes play a role of predecessors or fragments of polyelectrolyte gels. From a theoretical point of view, the properties of branched polymers and polyelectrolytes are different from those of their linear analogs because of the presence of an additional structural degree of freedom, *i.e.* the degree of branching. Variation in the degree of branching leads to a continuous change in the properties of branched macromolecules from nearly linear-like chains to soft nano-particles. In addition, some important biological polymers (for example, polysacharides) can be considered as branched weak polyelectrolytes [3]. Thus, investigation of the branched polyelectrolytes is also relevant for biophysical problems.

The simplest representative of regularly branched polymers is a star-branched macromolecule. Star-like polymers can also serve as a model for block copolymer micelles [4–6].

In our previous paper [7] we have analyzed conformations of star-branched polyelectrolytes as a function of the number of branches in dilute and semi-dilute salt-free solutions. In both systems, the screening of Coulomb interactions was provided by the counterions only. In this analysis we employed the analogy between charged branched polymers and polyelectrolyte brushes [8,9] as well as the idea of nonlinear screening in the macroion solution [10]. The charge of the macromolecule was assumed to be quenched, which corresponds to the case of strongly dissociating ionogenic groups in the chains.

The goal of the present paper is to extend our consideration to a salt-added solution and to analyze the effect of the ionic strength on the dimensions and intrinsic structure of the polyelectrolyte stars.

We also take into account the balance of the dissociation and recombination of charged monomers with the counterions. This process is most important for weak polyelectrolytes. As we see below, the interplay between the branched architecture and the dissociation-recombination equilibrium results in qualitatively novel features in the

[a] *Permanent address*: Institute of Macromolecular Compounds of the Russian Academy of Sciences, 199004, St. Petersburg, Russia
[b] e-mail: borisov@fenk.wau.nl

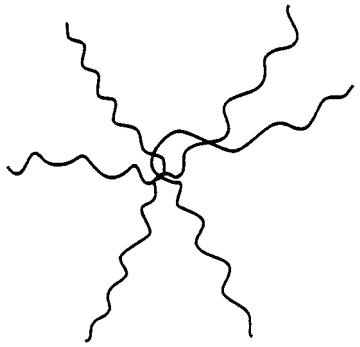

Fig. 1. Polyelectrolyte star with f branches; N is the number of monomer per branch.

behavior of branched polyelectrolytes in comparison to their linear analogs.

The paper is organized as follows. In Section 2 we introduce our model of star-branched polymers and polyelectrolytes and summarize the basic results for uncharged star polymers. In Section 3 we discuss the conformation of star-branched polyelectrolyte in a salt-free solution, focusing on the intrinsic structure of the macromolecule. Section 4 contains the analysis of conformational changes in a star polyelectrolyte induced by the addition of salt in the bulk solution. In Section 5 we consider stars with the annealed charge, *i.e.* we take into account the recombination-dissociation balance. Finally, Section 6 contains discussion and comparison with the available experimental data.

2 Star-branched polymers and polyelectrolytes

2.1 Model

In this section we introduce our model and discuss shortly the conformations of neutral star polymers following the lines of references [11–14].

We consider a dilute solution of star-branched macromolecules consisting of f arms each containing N monomer units (Fig. 1). We assume that the fraction α of charged monomer units in the chain is small and the Bjerrum length $l_B = e^2/k_BT\epsilon$, which characterizes the strength of the Coulomb interaction is of the order of a monomer unit length a. Here, e is the elementary charge, ϵ is the dielectric constant of the solvent, T is the temperature and k_B is the Boltzmann constant. The condition of weak charging implies that the energy of the Coulomb repulsion of any two neighboring (along the chain) charged monomers is much smaller than k_BT, *i.e.* $\alpha \ll (a/l_B)^2 \cong 1$. We consider an intrinsically flexible polyelectrolyte, *i.e.* the "bare" persistence length A of corresponding uncharged polymer is assumed to be of order of the monomer unit length a. As both conditions of weak charging and intrinsic flexibility apply, the Coulomb interactions do not lead to local stiffening of the star branches.

The total charge of the star-polyion is equal to $Q = ef\alpha N$. Due to the electroneutrality condition, the solution contains also counterions which, in total, compensate the overall charge of star-branched polyions. In this section we assume that no salt is added to the solution. Correspondingly, in the limit of zero polymer concentration, the Debye screening length tends to infinity.

The non-electrostatic, short-range interactions between the uncharged units are described by the dimensionless second, v, and the third, w, virial coefficients. The contribution of binary contacts is determined by the second virial coefficient, v, which grows linearly with temperature and vanishes in the θ-point, $v \cong (T-\theta)/T$. The contribution of ternary contacts is described by the third virial coefficient, w, which is virtually independent of T and is of the order of unity.

For simplicity, we assume that the non-electrostatic binary interactions between the uncharged units are weak, namely, the solvent is a θ-solvent. This assumption is reasonable because:

(i) the solubility of many synthetic polyelectrolytes in water (or other polar solvents) is ensured by the presence of charges on the chains, while for uncharged monomers, the solvent is marginally good or even poor;

(ii) in strongly branched polymers the repulsive short-range ternary interactions between uncharged monomers play an important role providing swelling of the branched chains in a θ-solvent [11–14].

2.2 Neutral stars

We start with a short review of the main results [11–15] on neutral stars under both, θ- and good solvent conditions.

The short-range repulsive interactions between units of different arms of the star lead to the extention of the arms in radial direction with respect to the dimension of isolated linear chains with the same number of monomers N. The equilibrium star dimension $R(f)$ is given by

$$R(f) \cong \begin{cases} N^{1/2} f^{1/4} a & \theta\text{-solvent} \\ N^{3/5} v^{1/5} f^{1/5} a & \text{good solvent.} \end{cases} \quad (1)$$

Because of the branched architecture of the molecule, the average intramolecular concentration of monomers is sufficiently large so that even under the θ-conditions, the repulsion due to ternary contacts ensures the swelling of the branches with respect to their Gaussian dimensions. The effect is comparatively weak and is manifested only at a relatively large number of branches (*i.e.*, for highly branched stars).

Equation (1) can be obtained by applying the mean field arguments. It results from the balance of the conformational free energy penalty for the extension of all f branches of the star,

$$F_{conf}(R)/k_BT \cong fR^2/Na^2 \quad (2)$$

and the free energy of short-range interactions between monomers (pair and ternary contacts),

$$F_{conc}(R)/k_BT \cong va^3(fN)^2/R^3 + (fN)^3a^6/R^6.$$

The intrinsic structure of the star polymer can be visualized by employing the blob picture according to which the neutral star is envisioned as a system of closely packed concentric spherical shells of blobs. The blob size is equal to the correlation length ξ_c which is determined by the local concentration of monomers ("concentration" blob). Locally, the star polymer is considered as a semi-dilute polymer solution of concentration $c(r)$ and the relationships between the local concentration and the correlation length are given by $\xi_c \cong (ca^3)^{-1}a$ or $\xi_c \cong (ca^3)^{-3/4}v^{-1/4}a$ for θ- or good solvent conditions, respectively [16]. (Here and below r is the distance from the center of the star.) The chain part inside the blob retains the unperturbed Gaussian or the excluded volume statistics so that the number of monomers g in a blob is related to its size as $\xi \cong g^{1/2}a$ or $\xi \cong g^{3/5}v^{1/5}a$, respectively. Each branch of the star contributes one blob to each concentric shell. The condition of close packing of the blobs in the shell of radius r implies the radial dependence of the blob size, $\xi_c(r) \cong rf^{-1/2}$, and the monomer density decay as

$$c(r) \cong a^{-3}\begin{cases} f^{1/2}(r/a)^{-1} & \theta\text{-solvent} \\ f^{2/3}v^{-1/3}(r/a)^{-4/3} & \text{good solvent.} \end{cases} \quad (3)$$

The normalization of the density profile described by equation (3) results in the same equation (1) for the overall star size that follows from the mean field arguments.

3 Polyelectrolyte star in salt-free solution

When the fraction of charged monomers in the star polyelectrolyte is small, the Coulomb interaction does not play an important role. As a result, the equilibrium conformation of the star is determined by the short-range repulsion between monomers (the so-called quasi-neutral behavior) and described by equations (1, 3).

If, however, the fraction of charged monomers is sufficiently large, the Coulomb repulsion between the charges results in an additional extension of the star branches in the radial direction. The equilibrium size of the star can be obtained by the balance of the energy of electrostatic repulsion

$$F_{Coulomb}/k_BT \cong l_B(\alpha fN)^2/R$$

and conformational free energy, equation (2), to give

$$R(f) \cong N\alpha^{2/3}(l_B/a)^{1/3}f^{1/3}a. \quad (4)$$

According to equation (4), all the branches in the polyelectrolyte star are extended proportionally to their degree of polymerization N (similar to a linear polyelectrolyte with the end-to-end distance $R(f=1) \cong N\alpha^{2/3}(l_B/a)^{1/3}a$ [17]), while the additional inter-arm Coulomb repulsion is described by the prefactor $f^{1/3}$. Comparison of equations (1, 4) shows that the long-range Coulomb repulsion causes stronger extension of the branches (with respect to the size of an isolated linear chain) than the short-range repulsion; the exponent in the f-dependence for a charged star size is noticeably larger than that for a neutral one.

Deriving equation (4) we have assumed that there is no screening of Coulomb interaction inside the star. This assumption can be justified in a dilute solution, where the average concentration of counterions is so small that the corresponding screening length is much larger than the star size.

It is remarkable, however, that according to equation (4), the size of a polyelectrolyte star grows with an increase in the number of branches in the star f *more slowly* than the total charge of the star $Q \sim f$. As a result, at large f the approximation of free counterions is not valid anymore and equation (4) fails. We expect that at large f, the star retains most of its counterions so that local concentration of counterions inside the star becomes much larger than the average concentration in the solution. This idea of charge renormalization has been proposed first for charged colloidal particles in salt-free solutions [10] and extended later to polyelectrolyte brushes [8,9], charged block-copolymer micelles [4–6] and branched polyelectrolytes [7]. Here we present only the result, while the detailed discussion can be found in [8,10] and (for the particular case of polyelectrolyte stars) in [7].

Because of the balance between the translational entropy of counterions and the Coulomb attraction of the counterions to the polyion, the counterions are never smeared uniformly in the volume of the solution but are localized preferentially in the region occupied by the star polyion. The number of counterions retained inside the star is determined by the ratio of the "bare" charge of the star, $Q = ef\alpha N$, and its size R. At $Q \ll eR/l_B$, the counterions are essentially free and the fraction of counterions localized inside the star is (in the dilute limit) small. This is the case for stars with small number of branches for which equation (4) is applicable. In the opposite limit, $Q \gg eR/l_B$, corresponding to many-arm stars, most of the counterions are trapped inside the star. In this regime, the intra-star Coulomb repulsion is strongly screened by the counterions and it is the osmotic pressure of counterions inside the star that gives the main contribution to the stretching force causing the swelling of the star branches. The balance between this osmotic force, $R^2\Delta\pi/k_BT \cong f\alpha N/R$, and the elastic force in the extended branches, $-\partial F_{conf}(R)/\partial R$, (where the conformational freee energy $F_{conf}(R)$ is given by equation (2)) results in the following dependence for the star size,

$$R(f) \cong N\alpha^{1/2}a. \quad (5)$$

The most remarkable feature of the many-arm stars is virtual independence (within the accuracy of a power law) of the star size of the number of branches f.

The crossover between the unscreened and the screened stars (referred below as "osmotic" stars) corresponds to the crossover between equations (4, 5) and occurs at $f \cong f^*$ where

$$f^* \cong \alpha^{-1/2}(l_B/a)^{-1}. \quad (6)$$

We see that only if the branches are weakly charged, $\alpha \ll 1$, then $f^* \gg 1$ and the unscreened regime can be observed.

As we see from equations (4, 5), both in the regime of unscreened Coulomb repulsion and in the osmotic regime, the branches of the polyelectrolyte star are extended proportionally to the number of monomers per branch. This implies that the monomer density decay in the radial direction is proportional to $\sim r^{-2}$, or more explicitly,

$$c(r) \cong a^{-3} \begin{cases} f^{2/3}\alpha^{-2/3}(l_B/a)^{-1/3}(r/a)^{-2} & f \ll f^* \\ f\alpha^{-1/2}(r/a)^{-2} & f \gg f^*. \end{cases} \quad (7)$$

Equation (7) implies uniform extension of the branches and has been also confirmed by the more detailed SCF calculations in [18].

3.1 Blob picture

In the frame of the blob picture, each branch can be envisioned as a string of Pincus stretching blobs [19] *of constant size*

$$R(f) \cong (N/g)\xi(f),$$

where the number of monomers per blob is $g \cong (\xi/a)^2$. The size $\xi(f)$ of each blob is inversely proportional to the local tension in the branch provided by the force of Coulomb repulsion or by osmotic pressure of counterions and is given by [7]

$$\xi(f) \cong \begin{cases} \alpha^{-2/3}f^{-1/3}(l_B/a)^{-1/3}a & f \ll f^* \\ \alpha^{-1/2}a & f \gg f^*. \end{cases} \quad (8)$$

In contrast to blobs in a neutral star, these blobs are not closely packed and their size does not depend on r. At $f = 1$, we arrive at a familiar result [17] for an individual polyelectrolyte chain, $\xi \cong \xi_0 \cong \alpha^{-2/3}(l_B/a)^{-1/3}a$. Increases in f lead to a decrease in ξ. At $f < f^*$, the unscreened Coulomb repulsion between branches leads to the reduction in ξ as $\xi = \xi_0 f^{-1/3}$. However, at $f \gg f^*$, screening of the inter-branch repulsions by the counterions prevents further decreases in ξ, and the size of electrostatic blob becomes independent of f. Here, the local structure of the branch is characterized by the relationship "one charge per blob".

One can get a complementary interpretation of $\xi(f)$ in the osmotic regime by employing the concept of intrinsic screening length, κ_i^{-1}. We define κ_i^{-1} as $\kappa_i^2 = l_B c_i$, where $c_i(r)$ is the average concentration of counterions at distance r from the center of the star.

In the osmotic regime, *i.e.* at $f \gg f^*$, the Coulomb repulsion inside the star is screened by counterions and the star is localy electroneutral on the scales larger than κ_i^{-1}, provided that $\kappa_i^{-1} \ll R(f)$.

Hence, we can apply the local electroneutrality approximation [21], according to which $c_i(r) \cong \alpha c(r)$. Correspondingly, we get with the account of equation (7) that $\kappa_i^2(r) \cong f\alpha^{1/2}(l_B/a)r^{-2}$, *i.e.* the local screening length grows with the distance from the star center as $\kappa_i^{-1}(r) \sim r$.

As the Coulomb interactions between the branches are unscreened on scales smaller than κ_i^{-1}, the number of branches participating in this unscreened repulsion can be estimated as $\kappa_i^{-2}(r)f/r^2 \cong f^*$, *i.e.* coincides with a number of branches f^* in the star at the threshold of the osmotic regime. Each such branch contributes a segment of $n(r)$ monomers into the screening volume $\kappa_i^{-3}(r)$. The balance of Coulomb repulsion of $f^*\alpha n(r)$ charged monomers localized within a volume $\kappa_i^{-3}(r)$ with the conformational entropy losses due to stretching of the chains, $f^*\kappa_i(r)^{-2}/n(r)a^2$, gives $n(r) \cong \kappa_i^{-1}(r)\alpha^{-1/2}a^{-1}$. Thus, we arrive at the size of the electrostatic blob $\xi \cong \alpha^{-1/2}a$.

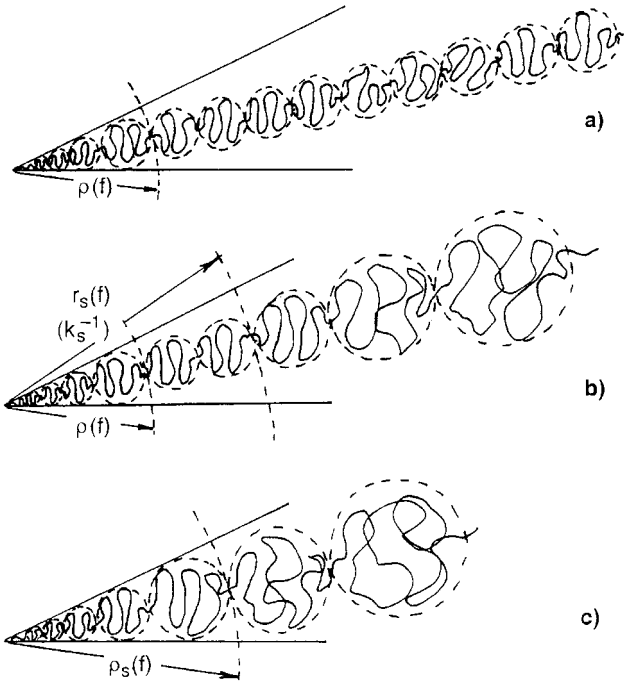

Fig. 2. The blob picture of a polyelectrolyte star with a quenched fraction of charged monomers in a salt-free solution (a) and in a salt-added solution (b, c); Figure (b) corresponds to the range of salt concentration where $\rho(f) \ll r_s(f)$ or $\rho(f) \ll \kappa_s^{-1}$ in cases $f \gg f^*$ and $f \ll f^*$, respectively. The outermost parts of chains consisting of blobs of constant size ξ_0 at $r \geq r^*$ are not shown.

Intrinsically, the polyelectrolyte star consists of two regions, Figure 2a (compare [20]). In the outer region, the extension of branches is determined by the Coulomb repulsion of charged monomers or/and by the osmotic pressure of counterions so that the branches are uniformly extended and are envisioned as the strings of blobs of constant size given by equation (8). The monomer density profile in this region is described by equation (7). In the inner (core) region, the local monomer density is sufficiently large and the non-electrostatic short-range interactions (ternary contacts under θ-condition) determine the local correlations. Hence, the structure of the core coincides with the structure of the neutral θ-star: the blobs are closely packed, their size grows with r as $\xi \cong rf^{-1/2}$, while the monomer density decreases according to equation (3).

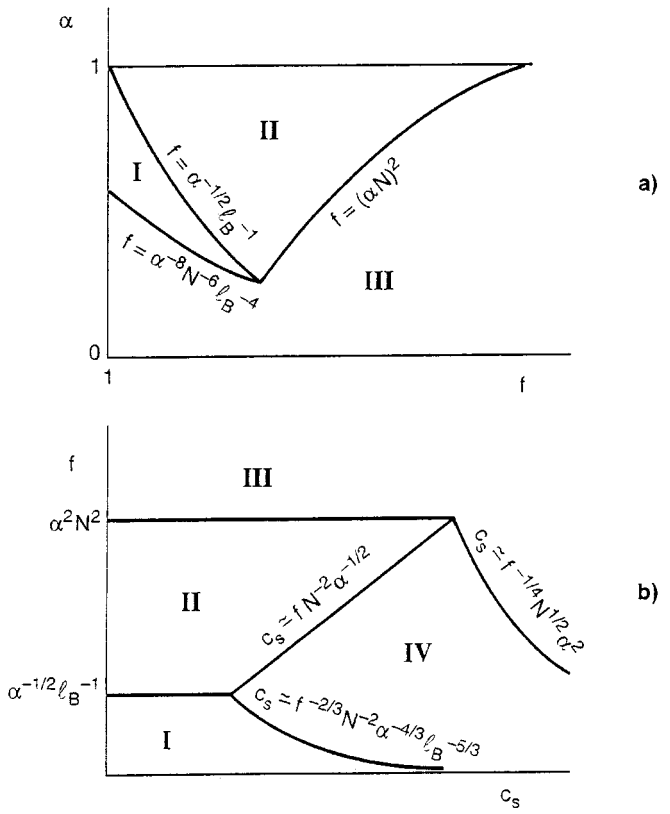

Fig. 3. The diagrams of states of a polyelectrolyte star with a quenched fraction of charged monomers: (a) in a salt-free solution; (b) in a salt-added solution, $\alpha \gg N^{-3/4}(l_B/a)^{-1/2}$. The regions of the diagram correspond to the star: (I) dominated by unscreened Coulomb repulsion of branches, (II) screened due to trapped counterions (osmotic regime), (III) dominated by non-electrostatic interactions between uncharged monomers (quasi-neutral regime), (IV) screened predominantly by co- and counterions of added salt.

The radius ρ of the θ-core can be determined from the condition of the crossover between the sizes of the concentration and the electrostatic blobs, $\xi(f) \cong f^{-1/2}r$, to give

$$\rho(f) \cong \begin{cases} af^{1/6}\alpha^{-2/3}(l_B/a)^{-1/3} & f \ll f^* \\ af^{1/2}\alpha^{-1/2} & f \gg f^*. \end{cases} \quad (9)$$

The condition $\rho(f) \cong R(f)$ determines the boundary between the polyelectrolyte regimes dominated by the Coulomb interaction or the osmotic pressure of counterions (at $f \ll f^*$ or $f \gg f^*$, respectively) and the regime of the quasi-neutral behavior of a star. Note, that in the osmotic regime the core radius $\rho(f)$ grows with f while $R(f) \cong const(f)$. Thus, an increase in the number of branches results in the transition to the quasi-neutral regime at $f \cong (\alpha N)^2$. In contrast, in the regime of predominance of the Coulomb repulsion, the core radius $\rho(f) \sim f^{1/6}$ *decreases* with a decrease in f more slowly than the overall radius of the star $R(f) \sim f^{1/3}$ so that transition to the quasi-neutral behavior occurs when the number of branches f is decreased. These features are demonstrated in the diagram of states presented in Figure 3a. The regions I and II of the diagram correspond to the star dominated by Coulomb interactions unscreened in regime I and partially screened by trapped counterions in regime II. Region III corresponds to the star dominated by non-electrostatic interactions between uncharged monomers (so-called quasi-neutral regime).

4 Polyelectrolyte star in salt-added solution

Up to now we considered only *salt-free* solution of polyelectrolyte stars, where the screening of electrostatic interactions was performed by the conterions that ensure the electroneutrality of the solution. In the limit of dilute solution, the *average* concentration of counterions is too small to provide screening of the Coulomb interactions on the scale of order of the star size [7]. We have seen however, that if the number of branches in a star is sufficiently large, *i.e.*, $f \gg f^*$, then the distribution of counterions in the solution becomes essentially non-uniform. Namely, most of the counterions are trapped inside the stars while the concentration of counterions in the inter-star regions is considerably smaller than the average value. This is a manifestation of the nonlinear screening effect in the solution of strongly branched polyelectrolytes.

Let us turn now to the case when 1:1 electrolyte, *e.g.* simple low molecular weight salt, is added to the solution of charged star polymers. We still consider a dilute solution of stars where the average concentration of charged monomers is much smaller than the concentration of added salt. In this situation, the Debye screening length κ_s^{-1} in the bulk of the solution is determined by the concentration c_s of added salt *via* the conventional relationship

$$\kappa_s^2 \cong l_B c_s.$$

It is convenient to start the analysis of the salt effect from polyelectrolyte stars with a large number of branches, $f \gg f^*$ (*i.e.*, the osmotic stars).

As we have discussed in Section 3, the many-arm star polyelectrolytes retain most of their counterions in the intra-star space even in a dilute salt-free solution. The average concentration of the counterions trapped inside the osmotic star is given by

$$c_i \cong \alpha f N/R^3(f) \cong fN^{-2}\alpha^{-1/2}a^{-3}. \quad (10)$$

An additional screening of intra-star Coulomb repulsion by the salt ions becomes important when the concentration c_s of added salt exceeds the internal concentration c_i of counterions in the osmotic star, or, equivalently, when the screening length κ_s^{-1} in the bulk of the solution becomes smaller than the "intrinsic" screening length κ_i^{-1}. At $c_s \gg c_i$ the screening inside the star is dominated by salt ions and we refer to this regime as to the salt dominated regime.

Because of the electroneutrality condition, the average concentration of counterions in the volume occupied by

the star polyion is always larger than their concentration c_s in the bulk of the solution while the average concentration of co-ions inside the star is smaller than c_s. The stretching force produced by screened Coulomb repulsion between the charged branches is proportional to the difference in the osmotic pressure of co- and counterions inside and outside the star. This force determines the swelling of the star branches and can be obtained by employing the local electroneutrality condition inside the star,

$$\alpha c + c_- = c_+ \tag{11}$$

(here the star branches are assumed to be charged negatively) and the Donnan rule for the distribution of co- and counterions

$$c_-/c_{b-} = c_{b+}/c_+ \tag{12}$$

where c_+, c_{b+} and c_-, c_{b-} are the concentrations of cations and anions inside the star, and in the bulk of the solution, respectively. The concentrations of co- and counterions in the bulk of the solution are equal, *i.e.* $c_{b-} = c_{b+} = c_s$. The differential osmotic pressure is given by

$$\Delta\pi/kT = \sum_j (c_j - c_{bj}) \cong \begin{cases} \alpha c & \alpha c \gg \sum_j c_{bj} \\ \alpha^2 c^2 / \sum_j c_{bj} & \alpha c \ll \sum_j c_{bj} \end{cases} \tag{13}$$

where in case of 1:1 added electrolyte $\sum_j c_{bj} = 2c_s$.

In the salt dominance regime (*i.e.*, at $c_s \gg c_i \cong \alpha c$), this differential osmotic pressure at the edge of the star is given by

$$\Delta\pi/k_BT \cong \alpha^2 c^2(R) c_s^{-1}$$

where the monomer concentration $c(R)$ is proportional to the average monomer concentration in the star fN/R^3. By balancing the total stretching force, $\Delta\pi R^2$, with the elastic force, $-\partial F_{conf}/\partial R$, (where the conformational free energy $F_{conf}(R)$ is still defined by Eq. (2)) we obtain the overall size of the star in the salt dominance regime

$$R_s(f) \cong N^{3/5} f^{1/5} \alpha^{2/5} (c_s a^3)^{-1/5} a. \tag{14}$$

As follows from equation (14), the addition of salt (an increase in c_s) leads to gradual deswelling of the polyelectrolyte star because of screening of the Coulomb repulsion between the charged branches. The screened Coulomb repulsion provides the same exponents for the molecular weight and the number of arms dependence of the star size as the short-range, excluded volume interactions under the good solvent conditions, equation (1). Equation (14) can be interpreted in terms of swelling of a polyelectrolyte star due to electrostatic excluded volume interactions, $R_s(f) \cong N^{3/5} f^{1/5} v_{eff}^{1/5} a$, with the corresponding effective second virial coefficient $v_{eff} \cong \alpha^2 (c_s a^3)^{-1}$. It is remarkable that the size of the osmotic ($f \gg f^*$) star in the *salt-free* solution, equation (5), can be formally obtained in the same way by setting $v_{eff} \cong \alpha^2 (c_i a^3)^{-1}$.

The crossover between equations (5, 14) corresponding to the onset of the salt-induced contraction of the star, occurs at $c_s \cong c_i \sim f$, *i.e.* when the salt concentration in the bulk of the solution becomes of the order of the counterion concentration inside the osmotic star. The latter is proportional to the number of branches, f. Hence, the larger is the number of branches in the star, the higher salt concentration is required to affect the star conformation.

4.1 Blob picture

In order to give insight to the intrinsic structure of the polyelectrolyte star in the salt dominance regime, we apply the condition of local balance of the differential osmotic force,

$$\Delta\pi(r) r^2/f k_BT \cong \alpha^2 c^2(r) r^2/f c_s$$

and the local tension $t(r)/k_BT$ in the star arms. As each arm exhibits locally Gaussian statistics, this local tension is proportional to the ratio of the radial elongation dr of the part dn of the arm, *i.e.* $t(r)/k_BT \cong dr/dn$. Under the condition of equal stretching of all the arms in the star, the local tension is related to the local monomer concentration *via* the equation

$$\frac{dr}{dn} \cong \frac{f a^3}{r^2 c(r)}\,. \tag{15}$$

As a result, we obtain the monomer density profile

$$c(r) \cong f^{2/3} (\alpha^{-2} c_s)^{1/3} a^{-2} (r/a)^{-4/3} \tag{16}$$

and the radial dependence of the blob size which is inversely proportional to the local tension in the branches,

$$\xi_s(r) \cong (f\alpha^2)^{-1/3} c_s^{1/3} (r/a)^{2/3}. \tag{17}$$

Equations (16, 17) can be obtained by using a different argument, *i.e.* by employing the concept of Debye screening length, κ_s^{-1}. At small distances from the star center r, where $\kappa_s^{-1} > \kappa_i^{-1}(r)$, the internal star structure is not affected by added salt. Here, one finds the core of radius $\rho(f)$ defined by equation (9) consisting of increasing θ-blobs surrounded by the strings of electrostatic blobs of size $\alpha^{-1/2} a$, see previous section. At $r \gg r_s(f) \cong f^{1/2} \alpha^{1/4} \kappa_s^{-1}$, the electrostatic interactions between the branches are screened on a scale larger than κ_s^{-1}. Here, the concentration of salt ions exceeds that of the counterions and screening is goverened by the salt. The dependence

$$r_s(f) \cong (f \alpha^{1/2} c_s^{-1} a^{-3})^{1/2} a \tag{18}$$

is determined by the equality of the local concentration of counterions, $\alpha c(r_s)$, in the osmotic star and the salt concentration, c_s, in the bulk solution.

Applying the same argument as in Section 3, we find that at $r \gg r_s$, only $f_s^* = f\kappa_s^{-2}/r^2$ branches contribute to the unscreened electrostatic interaction within the screening volume κ_s^{-3}. It is remarkable, that $f_s^* \sim r^{-2}$, *i.e.* in contrast to f^*, f_s^* decreases with increases in r, because $\kappa_s = const(r)$. Each branch contributes a segment of $n(r)$ monomers to the screening volume κ_s^{-3}. By balancing the

electrostatic force $\sim l_B f_s^*(\alpha n)^2/\kappa_s^{-2}$ with the elastic force $\sim \kappa_s^{-1}/na^2$ (per branch) we find for the local tension in the branch $t(r)/k_BT \cong \kappa_s^{-1}/na^2 \cong \alpha^{2/3} f^{1/3} c_s^{-1/3} (r/a)^{2/3}$. Correspondingly, we arrive at equation (17) for the size of electrostatic blob and to equation (16) for polymer profile.

The above picture holds in the range of r where $f_s^* > 1$. At $r \cong r^* \cong f^{1/2}\kappa_s^{-1}$, we have $f_s^* \cong 1$, while the distance between the branches equals κ_s^{-1}. Here, the size of electrostatic blob, $\xi_s(r)$, becomes equal to that in an individual polyelectrolyte chain, $\xi_0 \cong \alpha^{-2/3}(l_B/a)^{-1/3}a$ [17]. In other words, ξ_0 equals to the size of the largest segment of the polyelectrolyte chain which remains unperturbed by Coulomb repulsion of charged monomers and retains Gaussian statistics. On the scales larger than ξ_0 (but smaller than κ_s^{-1}) Coulomb repulsion results in extension of a polyelectrolyte chain in a string of ξ_0-blobs.

At distances $r \geq r^*$ from the center, the local structure of each branch coincides with that of an individual polyelectrolyte chain, *i.e.*, is determined by the intra-chain Coulomb repulsion and is unaffected by salt unless $\kappa_s^{-1} \gg \xi_0$. The branches in this outer region constitute strings of electrostatic blobs of size ξ_0 on scales below κ_s^{-1}, while at larger scales, they are envisioned as flexible chains with renormalized units of size κ_s^{-1}. These units interact with each other with the second virial coefficient ($\sim \kappa_s^{-3}$), *i.e.*, the renormalized chains exhibit the excluded volume statistics. As a result, we arrive at the same dependence (16) for the polymer profile at $r \gg r^*$ and at the dependence (14) for the star size.

Intrinsically, the polyelectrolyte star in a salt-added solution can be envisioned as consisting of a few concentric regions, Figure 2b.

In the inner region, $0 < r < \rho(f)$, the star structure is dominated by the short-range non-electrostatic repulsions between the uncharged monomers; the radius $\rho(f)$ of the inner region is still determined by equation (9); the closely packed blob structure, $\xi(r) \cong f^{-1/2}r$, and the monomer density profile $c(r) \sim r^{-1}$ in this region are the same as in a neutral star.

In the intermediate region, $\rho(f) < r < r_s(f)$, the local extension of branches is determined by the screened Coulomb repulsion, but the local concentration of counterions is much larger than the concentration of salt in the bulk of the solution; the screening of Coulomb interactions is dominated by counterions. The branches in this region are uniformly extended and consist of blobs of constant size, $\xi \cong \alpha^{-1/2}a$, each containing one charged monomer; the monomer density decreases as $c(r) \sim r^{-2}$, equation (7).

At $r_s < r < r^*$, the screening is dominated by the salt ions. Here, the size of electrostatic blob increases according to equation (17) due to screening of the inter-branch repulsion.

Finally, at $r \gg r^*$, the size of electrostatic blob is determined totally by the intra-branch interactions between the charges, and it stays constant, $\xi \cong \xi_0$, unless $\kappa_s^{-1} \leq \xi_0$.

As the salt concentration c_s in the bulk of the solution increases, the boundary r_s gets shifted towards the center of the star: the salt penetrates into the star and the width of the salt-dominated region ($r > r_s$) increases while the intermediate "osmotic" region shrinks (we remind that the size $\rho(f)$ of the θ-core remains virtually unaffected by an increase in the salt concentration). The extension of branches in the outer region and size of the star as a whole decrease according to equation (14) as well.

At $c_s \cong \alpha^{3/2}a^{-3}$, the crossover $r_s(f) \cong \rho(f)$ (where the radius $\rho(f)$ of the core is still determined by equation (9)) occurs, and the intermediate "osmotic" region disappears.

At larger salt concentrations, $\alpha^{3/2}a^{-3} \ll c_s \ll \alpha^{4/3}a^{-3}$, the star consists of the inner, θ-core dominated by short-range repulsion of uncharged monomers and the outer region dominated by screening by salt Coulomb repulsion between charged monomers, Figure 2c. The radius of the θ-core in this salt dominance regime is defined as

$$\rho_s(f) \cong f^{1/2}\alpha^{-2}c_s a^4. \tag{19}$$

This relationship is obtained by equating the sizes of a θ-blob, $\xi_c \cong r/f^{1/2}$, and the electrostatic blob determined by equation (17). The outer, salt dominated region of the star ($r > \rho_s$) consists of a sublayer of growing electrostatic blobs ($r \leq r^*$) and the sublayer with constant blob size (ξ_0) at $r \geq r^*$. As the salt concentration continues to increase, the Coulomb repulsion gets more and more screened, resulting in a decrease in the extension of the outer parts of branches (and in the star size as a whole) and simultaneously in an increase of the radius of the θ-core, equation (19).

At $c_s \cong \alpha^{4/3}a^{-3}$, the crossover $\rho_s(f) \cong r^*$, occurs and the sublayer of growing blobs disappears. Here, the salt-controlled screening length κ_s^{-1} becomes equal to the ξ_0, and at higher salt concentrations, the electrostatic blob is disrupted. Now, the interactions between monomers are described as the short-range binary repulsions between charged units. The corresponding second virial coefficient is $v \cong \alpha^2/c_s a^3$. The outer part of the star swells equivalently to a neutral star in a good solvent. The boundary between the swollen part of the star and the θ-core is determined by the condition of swelling of a θ-blob, to give the above expression for $\rho_s(f)$.

Eventually, at $c_s \cong \alpha^2 f^{-1/4} N^{1/2} a^{-3}$ the crossover $\rho_s(f) \cong R_s(f)$ occurs. At higher salt concentrations, the Coulomb repulsion is strongly screened all over the star which acquires the conformation of a neutral star polymer under θ-conditions. Here, the size of the star is given by equation (1).

The picture of salt-induced contraction of a polyelectrolyte star with a small number of branches, $f \ll f^*$, is slightly different from that described above. At low salt content, $\kappa_s^{-1} \gg R(f)$, as well as in a salt-free solution the intra-star Coulomb repulsion is not screened and the star conformation (described in Sect. 2) is not affected by this small amount of added salt. The screening effect of salt inside the star becomes important at $\kappa_s^{-1} \leq R(f)$ corresponding to the salt concentration $c_s \geq N^{-2} f^{-2/3} \alpha^{-4/3} (l_B/a)^{-5/3} a^{-3}$. At $\kappa_s^{-1} \ll R(f)$, the star is locally electroneutral so that the stretching force applied to the branches is proportional to the differential osmotic

pressure and the overall star size is described by equation (14). Intrinsically, the star is again subdivided into concentric regions. On the scale smaller than κ_s^{-1} from the center, screening effects are not important and the structure of a nonscreened star in a salt-free solution is retained. Here, the star consists of the θ-core of the radius $\rho(f)$ defined by equation (9) surrounded by the corona formed by uniformly extended branches, $r > \rho(f)$. At the larger distances from the center, $\kappa_s^{-1} < r < R_s(f)$, the screening due to the added salt becomes important. Here, at $\kappa_s^{-1} < r < r^*$, the electrostatic blobs grow in size according equation (17), while at $r \geq r*$, we have $\xi \cong \xi_0$. With increase in salt concentration, the width, $\kappa_s^{-1} - \rho(f)$, of the central region decreases because of the decrease in κ_s^{-1} at constant $\rho(f)$. At $c_s \cong \alpha^{4/3} f^{-1/3} (l_B/a)^{-1/3} a^{-3}$, the crossover $\kappa_s^{-1} \cong \rho(f)$ occurs and the intermediate region (dominated by the unscreened Coulomb repulsion) disappears. At larger salt concentrations, the structure of the star becomes similar to that of a many-arm star described above. Namely, further increases in the salt concentration result in an increase of the radius of the θ-core and the simultaneous decrease of the extension of branches in the outer region.

The diagram of states of a polyelectrolyte star in a salt added solution (Fig. 3b) contains in addition to regions I, II and III described already for the salt-free case the region IV where screening of intra-star Coulomb repulsion is governed by salt.

5 Effect of charge annealing in polyelectrolyte stars

In previous sections we considered polyelectrolyte stars with *quenched* regular distribution of the charged monomers. In other words, we assumed the fraction of charged monomers and their uniform distribution along the branches of the star to be fixed and independent of the external conditions. This model is applicable for a regular copolymer with a fraction α of strongly dissociating monomers and a fraction $(1 - \alpha)$ of neutral monomers.

Another important example of weakly charged polyelectrolytes is weakly dissociating polyacids (or polybases) in which all the monomers are capable of ionization, but only a small fraction are actually ionized. The local ionization-recombination balance, *i.e.* the average fraction of ionized monomer units is determined by the ionization constant, K, and by the local concentration of counterions $c_{\mathrm{H}^+}(r)$ (H^+ ions in case of weak polyacid, which we consider below) *via* the mass action law

$$\frac{\alpha(r)}{1-\alpha(r)} = \frac{K}{c_{\mathrm{H}^+}(r)} \,. \tag{20}$$

The concentration $c_{b\mathrm{H}^+}$ of H^+-ions in the bulk of the solution depends not only on the average concentration of polyacidic stars, but can be also tuned by the variation of the pH of the solution, and determines the degree of dissociation of monomers of polyacid $\alpha_b \cong K/c_{b\mathrm{H}^+} \ll 1$ in the bulk of the solution. The last inequality corresponds to the condition of weak ionization.

5.1 Annealed polyelectrolyte star in salt-free solution

As the concentration of counterions (H^+ ions in case of polyacid) inside the star is larger or much larger than that in the bulk of the solution, the degree of ionization of branches is equal to or smaller than $\alpha_b \cong K/c_{b\mathrm{H}^+}$. The former is the case for the stars with a small number of branches $f \ll f^* \cong \alpha_b^{-1/2} (l_B/a)^{-1}$, that are unable to retain counterions. Average concentration of H^+-ions inside such stars is of the order of $c_{b\mathrm{H}^+}$. When the corresponding Debye screening length $\kappa_b^{-1} \cong (l_B c_{b\mathrm{H}^+})^{-1/2}$ is much larger than the star size [23], the Coulomb repulsion between the branches is not screened, and the branches are extended up to

$$R(f) \cong N \alpha_b^{2/3} (l_B/a)^{1/3} f^{1/3} a \tag{21}$$

(compare Eq. (4)). An increase in the number of branches does not result in a significant increase in the concentration of counterions inside the star. As a result, the degree of ionization α stays virtually unaffected, *i.e.*, $\alpha \cong \alpha_b$, as long as the number of branches remains smaller than $f^* \cong \alpha_b^{-1/2} (l_B/a)^{-1}$. At $f \geq f^*$, the counterions are strongly attracted by the star polyion and most of them do not leave the volume occupied by the star (see discussion in Sect. 3). Each branch contributes αN counterions. At the same time the size of the star in this "osmotic" regime is virtually independent of the number of branches or at least grows weaker than a power function of f. As a result, we expect that at a large number of branches, the counterion concentration c_{H^+} inside the star exceeds significantly the bulk value, $c_{b\mathrm{H}^+}$, giving rise to the recombination process.

In order to estimate the number of branches $\tilde{f}^*$ in the star corresponding to the onset of recombination we have to compare the intra-star concentration of counterions c_{H^+}, equation (10), where the size of the osmotic star $R(f) \cong N \alpha^{1/2} a$ is calculated at $\alpha \cong \alpha_b$ and the bulk concentration of counterions $c_{b\mathrm{H}^+}$. The intra-star concentration becomes larger than the bulk value at $f \gg \tilde{f}^*$ where

$$\tilde{f}^* \cong N^2 \alpha_b^{1/2} c_{b\mathrm{H}^+} \cong N^2 \alpha_b^{-1/2} K a^3. \tag{22}$$

At $f \gg \tilde{f}^*$, the degree of ionization of the star is determined by the intra-star concentration of counterions, $\alpha \cong K/c_{\mathrm{H}^+}(\alpha)$, which in turn depends on α *via* equation (10). After simple algebra we obtain the following dependence for the average degree of dissociation

$$\alpha(f) \cong (K a^3 N^2 f^{-1})^2 \tag{23}$$

and the overall star size

$$R(f) \cong N \alpha^{1/2}(f) a \cong N^3 K a^4 f^{-1}. \tag{24}$$

A remarkable consequence of equations (23, 24) is that the average degree of ionization of the star branches decreases with increasing f, that results, in turn, in the decrease of the overall star size. This behavior is qualitatively opposite

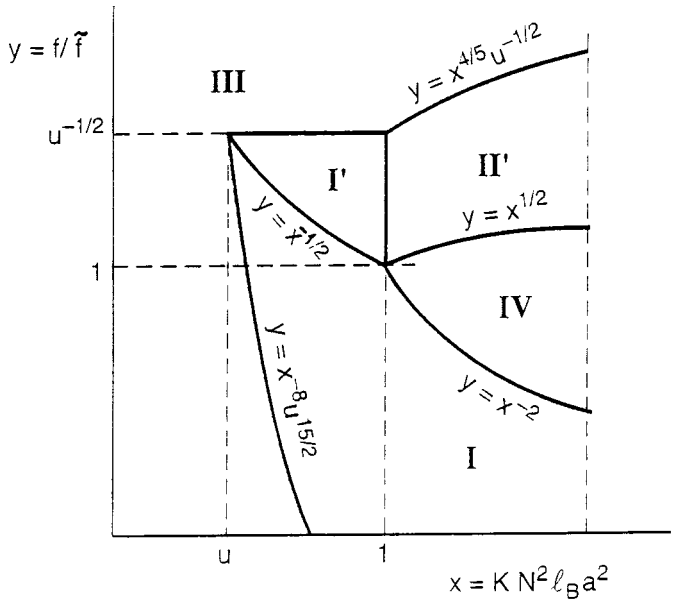

Fig. 4. The diagram of states of an annealed polyelectrolyte star in a salt-free solution in $x = KN^2a^2l_B, y = f/\tilde{f}$ coordinates; $\tilde{f} \cong f^*(x = 1) \cong c_{b+}^{1/2} N l_B^{-1/2} a^2$, $u \cong c_{b+} a^3 N^{6/5} (l_B/a)^{3/5} \leq 1$; regions I′ and II′ correspond to annealing unscreened and annealing osmotic regimes, respectively, while the right boundary of the diagram is determined by the condition $\alpha_b \leq 1$.

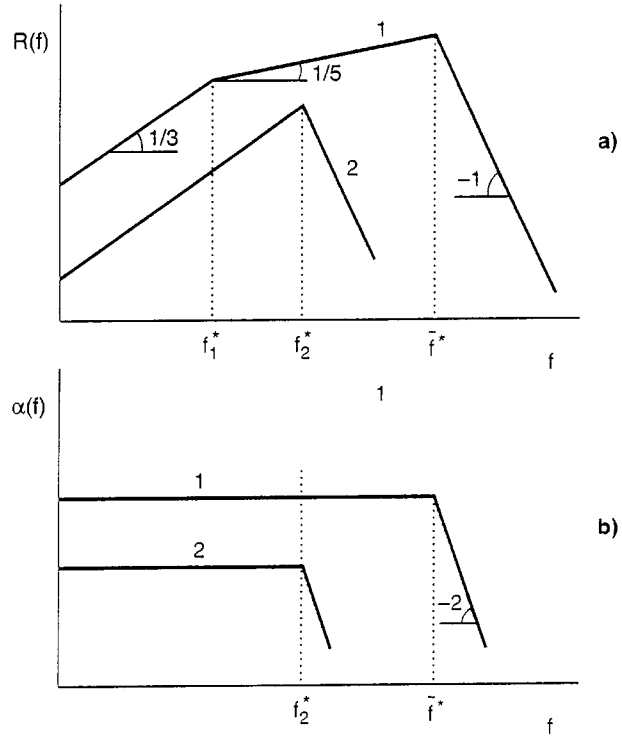

Fig. 5. Schematic dependence of the size (a) and of the degree of ionization (b) of an annealed polyelectrolyte star on the number of branches f for $KN^2a^2l_B \gg 1$, curve 1, and for $KN^2a^2l_B \ll 1$, curve 2.

to that described above for neutral or polyelectrolyte stars with quenched charge. The similar effect of decrease in the chain's extension with increasing grafting density has been predicted earlier for weak polyelectrolyte brushes of different morphologies [20,24].

Equation (22) can be rewritten as $\tilde{f}^* \cong f^* N^2 a^2 K l_B$ thus indicating that the onset of recombination occurs in the osmotic regime (*i.e.* $\tilde{f}^* \gg f^*$) only if the ionization constant K is sufficiently large, $N^2 K a^2 l_B \gg 1$.

If the same condition, $f \geq \tilde{f}^* \cong f^* N^2 K l_B$, is applied to define the onset of charge recombination in the star with small ionization constant, namely, $N^2 K l_B \ll 1$, we come to a contradiction, $\tilde{f}^* \ll f^*$. The underlying physics as follows: at small values of ionization constants, the intrinsic concentration of counterions at the charge renormalization threshold, $f \cong f^*$, appears to be sufficient to induce recombination that in turn must reduce the bare star charge below the threshold value required to retain counterions inside, *i.e.* to induce the renormalization of the star charge.

Therefore, in the frame of our scaling-type approach we can claim that as the number of branches increases over f^*, the recombination of charged monomers with the counterions keeps the star at the threshold of charge renormalization, *i.e.* the star size and the degree of ionization are determined simultaneously by the condition $R(f) \cong fN\alpha l_B$ and by any of equations (4) or (5).

As a result, we find that both the degree of ionization and the star size decrease with increasing number of branches f, ($f \gg f^*$), as

$$\alpha(f) \cong f^{-2} (l_B/a)^{-2} \tag{25}$$

and

$$R(f) \cong N f^{-1} (l_B/a)^{-1} a. \tag{26}$$

It is remarkable that the exponents in the f-dependences of the degree of ionization and of the star size in equations (25, 26) are the same as in equations (23, 24) respectively.

Due to an additional variable (*i.e.*, the degree of ionization α) the overall behavior of the annealed stars becomes more sophisticated than that of the quenched stars. As a result, the diagrams of states of the annealed stars become more varied. Figure 4 shows an example of such a diagram for the particular range of parameters, $c_{b+} a^3 N^{6/5} (l_B/a)^{3/5} \ll 1$, and $Na \gg \kappa_b^{-1}$, while Figure 5 shows the schematic dependences of the annealed star size on the number of branches f for large values of K ($K \gg (N^2 a^2 l_B)^{-1}$, curve 1) and small values of K ($K \ll (N^2 a^2 l_B)^{-1}$, curve 2). In addition to regions I, III, and IV described for the quenched charge case, the diagram of annealed polyelectrolyte star contains regions I′ and II′. The latter ones correspond to annealing unscreened and annealing osmotic regimes, respectively.

As follows from the diagram, at small number of branches, the degree of ionization of monomers in the star

is the same as in the bulk of the solution, $\alpha \cong \alpha_b$. Here, the usual unscreened star behavior is observed. In the opposite limit of large number of branches, the degree of ionization is much smaller than α_b, and the non-electrostatic intramolecular interactions predominate over electrostatic ones (quasi-neutral behavior).

The behaviour of the star at intermediate values of f depends strongly on the value of the ionization constant K.

In case of very weak polyelectrolyte, $K \ll (N^2 a^2 l_B)^{-1}$, the recombination of counterions becomes important even for the stars with the number of branches $f \geq f^* \cong \alpha_b^{-1/2}(l_B/a)^{-1}$. With further increases in f, the recombination keeps the star at the charge renormalization threshold.

The picture is different for strongly dissociating polyelectrolyte stars, $K \gg (N^2 a^2 l_B)^{-1}$. In this case, an increase in the number of branches brings the star into the screened regime, $R(f)\kappa_b \gg 1$, before the recombination of counterions becomes important. Further increase in f results in an increase of the concentration of counterions inside the star and finally reaches the recombination threshold at $f \cong f^* N^2 K a^2 l_B$. The star passes into the annealed osmotic regime when the extension of branches decreases with an increase in f because of massive recombination of the counterions with the charged monomers.

At larger values of the bulk concentration of H^+-ions (lower pH range) or at larger N, we have $c_{b+} a^3 N^{6/5}(l_B/a)^{3/5} \geq 1$. Correspondingly, regions I′ and II′ where recombination of charges is important disappear from the diagram of states and the star behaves as if with a quenched charge.

5.2 Blob picture

The intrinsic structure of annealed polyelectrolyte stars is characterized by the profiles of polymer and the counterion densities, the radial distribution of local tension in the branches and, additionally, by the profile of local degree of ionization of monomers.

At $f \gg \tilde{f}^*$, when the recombination of charges becomes important, all these distributions are determined self-consistently. Since the star as a whole is found in the osmotic regime, we can use the local force balance argument,

$$\frac{dr}{dn} \cong \alpha^{1/2}(r)$$

and the local ionization balance argument,

$$\alpha(r) \cong K/c_{H^+}(r)$$

together with the condition of local electroneutrality

$$c_{H^+}(r) \cong \alpha(r) c(r)$$

where the monomer density profile $c(r)$ and the local tension in the star arms dn/dr are interconnected by equation (15).

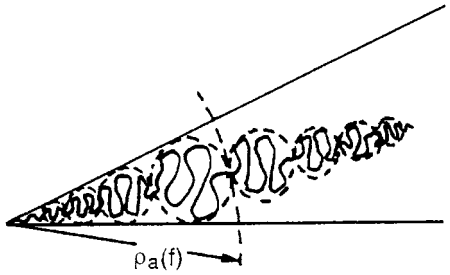

Fig. 6. The blob picture of a polyelectrolyte star with annealed fraction of charged monomers in the annealing osmotic regime (region II′ in the diagram of states, Fig. 4).

We remark that the same type of arguments were used earlier in [20] for the analysis of the intrinsic structure of annealed osmotic polyelectrolyte brushes.

As a result, we find

$$c(r) \cong f^{4/3}(Ka^3)^{-1/3}(r/a)^{-8/3}a^{-3} \quad (27)$$

$$\alpha(r) \cong f^{-2/3}(Ka^3)^{2/3}(r/a)^{4/3} \quad (28)$$

$$\xi(r) \cong dn/dr \cong f^{1/3}(Ka^3)^{-1/3}(r/a)^{-2/3}a \quad (29)$$

$$c_{H^+}(r) \cong f^{2/3}(Ka^3)^{1/3}a^{-2}(r/a)^{-4/3}a^{-3}. \quad (30)$$

As follows from equations (27, 28, 29, 30), the intrinsic structure of the annealing polyelectrolyte star in the osmotic regime is qualitatively different from that of a star with a quenched charge.

Because of the radial decrease in the concentration of counterions, the local degree of ionization of branches increases from the center to the periphery of the star, $\alpha(r) \sim r^{4/3}$. As a result, the local tension in the branches simultaneously increases that is manifested in the radial decrease of the blob size, $\xi(r) \sim r^{-2/3}$, The latter observation is in pronounced contrast to the size of blobs in neutral and polyelectrolyte stars with quenched charge, Figure 2. As the branches get locally more extended with an increase in r, the concentration of monomers decays more rapidly, *i.e.*, as $c(r) \sim r^{-8/3}$ (compare with $c(r) \sim r^{-2}$ dependence in quenched polyelectrolyte stars where the branches are uniformly extended).

The blob picture of the osmotic annealed polyelectrolyte star is presented in Figure 6. The most striking feature of the blob structure is the nonmonotonic dependence of the blob size on the distance from the center of the star: in the inner θ-core region, $0 < r < \rho_a(f)$, the blobs grow with r while in the osmotic region, $\rho_a(f) < r < R(f)$, described by equations (27–30), the blob size decreases with increases in r as described by equation (29). The radius $\rho_a(f)$ of the inner θ-core in the annealed polyelectrolyte

star defined by the crossover between the monomer density or the blob size profiles, is given by

$$\rho_a(f) \cong f^{1/2}(Ka^3)^{-1/5}a. \tag{31}$$

With increasing number of branches f the size of the θ-core increases, while extension of branches in the corona region decreases (Eq. (24)), and the star as a whole approaches the quasi-neutral regime.

5.3 Effect of added salt on the annealed polyelectrolyte star conformation

The addition of 1:1 salt to the solution of weak polyacid stars results in the screening of Coulomb repulsion between charged branches. If the concentration of H^+-ions inside the star is comparable to its bulk value, c_{bH^+}, then the degree of ionization of the star branches is equal to α_b. In this case, the size of the star decreases with an increase in salt concentration just as in the case of polyelectrolyte stars with quenched fraction of charged monomers described in Section 4. However, qualitatively opposite effect of added salt is expected for weak polyacid stars with large number $f \gg f^* N^2 K a^2 l_B$ of branches. In these star polyelectrolytes, the intrinsic concentration of counterions is much larger than that in the bulk solution. The addition of salt results in progressive substitution of H^+ -ions inside the star by the salt cations that leads to a decrease in the intrinsic concentration of H^+-ions. As a result, the recombination-dissociation balance gets shifted and the degree of ionization of the star branches increases thus giving rise to the star swelling as the ionic strength of the bulk solution increases.

In order to describe the effect of salt on the degree of ionization, we combine the mass action law, equation (20), with the local electroneutrality condition inside the star, equation (11), and the Donnan rule, equation (12), for the distribution all species of co- and counterions, where now $c_- = \sum_{j-} c_{j-}$ and $c_+ = \sum_{j+} c_{j+}$ and c_{j+}, c_{bj+} and c_{j-}, c_{bj-} are the concentrations of cations (H^+- and s^+-ions) and anions (OH^-- and s^--ions) inside the star and in the bulk of the solution, respectively. The relation $c_{bs-} = c_{bs+} = c_s$ still applies.

As a result, we obtain the equation for the degree of ionization,

$$\alpha \cong \alpha_b^{1/2}\left(\frac{c_{bs^+} + c_{bH^+}}{c}\right)^{1/2}, \tag{32}$$

which is valid at $c_{bs^+} + c_{bH^+} \ll \alpha c$, *i.e.* in the annealing osmotic regime. In the opposite limit, the degree of ionization of the star branches coincides with the bulk value, $\alpha \cong \alpha_b$. Equation (32) must be coupled to the relationship between the monomer concentration and the degree of ionization in the osmotic star, $c \cong fN^{-2}\alpha^{-3/2}a^{-3}$. As a result, we get

$$\alpha(f, c_s) \cong \alpha_b^2 N^4 f^{-2}(c_{bs^+} + c_{bH^+})^2 a^6 \tag{33}$$

and the star size scales as

$$R(f, c_s) \cong Na\alpha^{1/2}(f, c_s) \cong N^3\alpha_b f^{-1}(c_{bs^+} + c_{bH^+})a^4 \cong N^3 f^{-1}(\alpha_b c_s + K)a^4. \tag{34}$$

Hence, at given concentration of H^+-ions in the bulk of the solution, c_{bH^+}, the size of the star grows linearly with increasing c_s due to the substitution of H^+-ions by s^+-ions and corresponding additional ionization of the star branches. The effect becomes more pronounced at $c_s \gg c_{bH^+}$. We remind the reader that this effect of abnormal swelling of a polyelectrolyte star caused by an increase in the ionic strength of the solution takes place only at relatively low salt concentration c_s, when the total concentration of all types of counterions in the bulk of the solution remains much smaller than their concentration inside the osmotic star. As c_s becomes comparable to αc, the degree of ionization $\alpha(f, c_s)$ reaches the bulk value α_b, and further increase in c_s results in screening of electrostatic interactions and in deswelling of the star according to equation (14). Hence, the star dimension depends non-monotonically on c_s passing through the maximum at $c_s \cong fN^{-2}\alpha_b^{-2}a^{-3}$.

6 Discussion and conclusions

In this paper, we have analyzed the conformations of weak star-branched polyelectrolytes in dilute solution as a function of the number of branches f and of the salt concentration c_s.

The most important feature of many-arm polyelectrolyte stars in a dilute salt-free solution is essentially non-uniform distribution of the counterions. Most of them are localized preferentially (almost completely at large f) inside the stars. Hence, the local concentration c_i of counterions in the region occupied by a star polyion is much larger than their average concentration in the solution. As a result, the intra-star Coulomb repulsion between the charged monomers is strongly screened even in a dulite regime.

The effect of the ionic strength of the solution (tuned by the addition of low molecular weight salt) is different for weakly charged polyelectrolyte stars with a quenched fraction of strongly dissociating monomers (like PSSNa at low degree of sulphonation) and for weakly dissociating branched polyacids (or polybases).

An addition of salt to the solution of strongly branched *quenched polyelectrolyte stars* does not affect (up to a certain level) their conformation. Only when the bulk salt concentration exceeds the intrinsic concentration of the counterions, c_i, a noticeable deswelling of the star due to additional screening of the Coulomb repulsion between the charged branches can be observed. The greater the number of branches in a star, the higher the characteristic salt concentration required to induce the polyelectrolyte star contraction.

This conclusion is in agreement with recent experimental results of J. Mays, who employed the photon

correlation spectroscopy method [25] to measure the hydrodynamic radii of star-branched potassium polystyrenesulphonates (the number of branches was varied from 13 to 18) as a function of the ionic strength of the solution. In these experiments, the degree of sulphonation which determines the fraction of charged monomers was sufficiently high (close to 1). According to our analysis, such stars retain extension of their branches in a wider range of salt concentrations than the linear polyelectrolytes. The experiments of J. Mays, indeed, demonstrated relative insensitivity of the many-arm polyelectrolyte stars to an increase in the ionic strength of the solution in comparison to the corresponding linear polyelectrolytes.

Our results indicate that the addition of salt to the solution induces the rearrangement of the intrinsic structure of star-branched polyelectrolytes. We have shown that irrespective of the ionic strength of the solution, the central region (the θ-core) of the star is dominated by the non-electrostatic short-range repulsion between the uncharged monomers, and is envisioned as a system of closely packed concentration blobs. This dense central region is surrounded by Coulomb repulsion (or due to osmotic pressure of counterions) swollen corona and this corona determines the size of the star as a whole.

In a salt-free solution, the branches in the corona are extended uniformly and can be described as strings of elastic Pincus blobs of equal size; these blobs are not closely packed!

With increases in salt concentration, the salt ions penetrate preferentially into the sparse peripherical region of the corona and screen the electrostatic interactions there. The radial decay of the monomer density, $c(r)$, in this region is described by the same exponent as in a neutral star with the short-range excluded volume interactions (under good solvent conditions). However, in contrast to neutral stars, the elastic blobs in partially screened polyelectrolyte stars are not closely packed.

At the first stage of the salt-induced contraction, an increase in c_s and penetration of salt in the star results in shrinking of the intermediate region characterized by the uniform extension of branches but does not affect the radius of the θ-core. At higher salt concentrations, corresponding to the second stage of the contraction, the radius of the θ-core increases simultaneously with a decrease in the size of the corona.

In both cases, the overall size R of the star is governed by the outer part of the corona, $R(f, c_s) = N^{3/5}\alpha^{2/5}f^{1/5}(c_s a^3)^{-1/5}a$. We note that our results on salted stars are essentially different from the results of Dann and Tirrell [26]. Those authors considered the case of strongly charged, $\alpha \cong 1$, polyelectrolyte chains grafted to a planar and also to a spherical surface in a salt dominance regime. In the latter case, one could expect an exponent in the dependence of the grafted chain size, R, on the salt concentration c_s, similar to that found for the polyelectrolyte stars. However, there is a major discrepancy between our results and the findings in reference [26]. Our model predicts $R(f, c_s)$ proportional to $c_s^{-1/5}$, whereas the model of Dann and Tirrell gives R proportional to $c_s^{-2/5}$. The difference in the exponents has several sources. First of all, the authors of reference [26] focused on strongly charged polyelectrolytes where direct interactions between the charges on the chain provide the electrostatic stiffening of polyelectrolyte. The dependence of the electrostatic persistence length, L_e, on salt concentration still remains a "hot" point at the moment. The popular predictions $L_e \sim \kappa_s^{-2}$ [27] *versus* $L_e \sim \kappa_s^{-1}$ [28] are still under intensive discussion. Whereas the former one is proved to be applicable to strongly charged and/or intrinsically stiff polyelectrolytes, the latter seems to be more appropriate for flexible, weakly charged polylectrolytes. The results of our model can be reformulated in terms of electrostatic persistence length scaling as $L_e \sim \kappa_s^{-1}$ (see our previous work [22]). Authors of [26] employed the dependence $L \sim \kappa_s^{-2}$ to incorporate electrostatic effects into their model. They envisioned polyelectrolyte chain as consisting of stiff segments of length $\sim L_e$ and thickness a, and utilized the results of a scaling model for neutral semi-flexible polymer brushes. However, they did not take into account the important fact that electrostatic interactions renormalize not only the length of the segment, $L_e \sim \kappa_s^{-2}$ but the thickness of the segment as well. Namely, instead of monomer size a, the thickness of stiff segment becomes $\sim \kappa_s^{-1}$. Correspondingly, the excluded volume statistics changes, and instead of the dependence $R \sim c_s^{-2/5}$ obtained by Dan and Tirrel one gets $R \sim c_s^{-3/10}$. The latter dependence is expected for strongly charged polyelectrolyte stars in a salt dominance regime.

In case of *weakly dissociating (annealed) polyelectrolyte stars* the effect of added salt is essentially different from that in the quenched case. Small concentrations of salt induce additional swelling of the star. The origin of this effect is the shift of the ionization-recombination balance inside the star and the corresponding increase in the fraction of charged monomers. As the salt concentration increases beyond a certain level, the degree of dissociation reaches its maximal (*i.e.*, bulk) value, and the screening effect of salt becomes dominant resulting in deswelling of the star. Hence, the dependence of the weakly dissociating polyelectrolyte star on the ionic strength of the solution appears to be nonmonotonic and exhibits a maximum.

The intrinsic structure of weakly dissociating polyelectrolyte star is characterized by nonmonotonic dependence of the local tension in the star branches and of the elastic blobs size on the distance from the center of the star. The blob size increases with r in the central θ-core region, but *decreases* in the peripheric, osmotic region due to an increase in the local degree of dissociation (and in the local tension) with increasing distance from the center.

The experimental probe of the salt-induced structural changes in the polyelectrolyte stars could be performed by using SANS methods.

We are thankful to Prof. J.W. Mays for drawing our attention to experimental results on branched polyelectrolytes. O.V. Borisov appreciates the hospitality of Prof. G. Fleer and Prof. M. Cohen Stuart in the University of Wageningen and the NWO research grant. E.B. Zhulina acknowledges the

hospitality of Prof. A.C. Balazs at the University of Pittsburgh (USA). This work was partially supported by NWO Dutch-Russian program for Agricultural and Food Research.

References

1. F. Oosawa, *Polyelectrolytes* (Dekker, NY, 1971).
2. J.-L. Barrat, J.-F. Joanny, *Advances in Chemical Physics* **94**, edited by I. Prigogine, S.A. Rice (John Wiley, 1996).
3. A.L. Lehninger, *Biochemistry* (Worth Publishers, Inc., NY, 1979).
4. J.F. Marko, Y. Rabin, Macromol. **25**, 1503 (1992).
5. J. Wittmer, J.F. Joanny, Macromol. **26**, 2691 (1993).
6. P. Guenoun, S. Lipsky, J.W. Mays, M. Tirrel, Langmuir **12**, 1425 (1996); P. Guenoun, H.T. Davis, M. Tirrel, J.W. Mays, Macromol. **29**, 3965 (1996); P. Guenoun, Delsanti, D. Gazeau, J.W. Mays, D.C. Cook, M. Tirrel, L. Auvray, Eur. Phys. J. B **1**, 77 (1998).
7. O.V. Borisov, J. Phys. II France **6**, 1 (1996).
8. P. Pincus, Macromol. **24**, 2912 (1991); R. Ross, P. Pincus, *ibid.* **25**, 1503 (1992).
9. O.V. Borisov, T.M. Birshtein, E.B. Zhulina, J. Phys. II France **1**, 521 (1991); in *Modern Problems of Physical Chemistry of Macromolecules* (Cent. Bio. Res., Puschino, USSR, 1991), p. 85.
10. S. Alexander, P.M. Chaikin, P. Grant, G.J. Morales, P. Pincus, D. Hone, J. Chem. Phys. **80**, 5776 (1984).
11. M. Daoud, J.P. Cotton, J. Phys. France **43**, 531 (1982).
12. E.B. Zhulina, Polym. Sci. USSR **26**, 794 (1984).
13. T.M. Birshtein, E.B. Zhulina, Polymer **25**, 1453 (1984).
14. T.M. Birshtein, E.B. Zhulina, O.V. Borisov, Polymer **27**, 1078 (1986).
15. E.B. Zhulina, O.V. Borisov, T.M. Birshtein, Polym. Sci. USSR **30**, 780 (1988); E.B. Zhulina, O.V. Borisov, V.A. Pryamitsyn, T.M. Birshtein, Macromol. **24**, 140 (1991).
16. P.-G. de Gennes, *Scaling Concepts in Polymer Physics* (Cornell University Press, Ithaca, 1979).
17. P.-G. de Gennes, P. Pincus, R.M. Velasco, F. Brochard, J. Phys. France **37**, 1461 (1976).
18. O.V. Borisov, E.B. Zhulina, J. Phys. II France **7**, 449 (1997).
19. P. Pincus, Macromol. **10**, 210 (1977).
20. E.B. Zhulina, O.V. Borisov, Macromol. **29**, 2618 (1996).
21. E.B. Zhulina, O.V. Borisov, T.M. Birshtein, J. Phys. II France **2**, 63 (1992).
22. O.V. Borisov, E.B. Zhulina, T.M. Birshtein, Macromol. **27**, 4795 (1994).
23. The latter relation is valid at neutral or low pH that will be the case in our analysis.
24. E.B. Zhulina, T.M. Birshtein, O.V. Borisov, Macromol. **28**, 1491 (1995).
25. J.W. Mays, Polymer Commun. **31**, 170 (1990).
26. N. Dan, M. Tirrel, Macromol. **26**, 4310 (1993).
27. T. Odijk, J. Polym. Sci. **15**, 477 (1977); J. Skolnick, M. Fixman, Macromol. **10**, 944 (1977); A.R. Khokhlov, K.A. Khachaturian, Polymer **23**, 1742 (1982).
28. J.-L. Barrat, J.-F. Joanny, Europhys. Lett. **24**, 333 (1993).